JSHC
Japan Society of Histochemistry and Cytochemistry
Established 1959

Acta Histochem. Cytochem. 44 (4): 175–182, 2011
doi:10.1267/ahc.11005

Aquaporin 4 Expression in the mdx Mouse Diaphragm

Hajime Hara[1], Yoshihiro Wakayama[1], Hiroko Kojima[1], Masahiko Inoue[1], Takahiro Jimi[1], Shoji Iijima[1] and Hisatsugu Masaki[1]

[1]*Department of Neurology, Showa University Fujigaoka Hospital, 1–30 Fujigaoka, Aoba-ku, Yokohama 227–8501, Japan*

Received January 24, 2011; accepted June 23, 2011; published online August 4, 2011

Expression of aquaporin (AQP) 4 in the surface membranes of skeletal myofibers is well established; however, its functional significance is still unknown. The alterations of AQP4 expressions in dystrophic muscles at RNA and protein levels have been reported in various dystrophic muscles such as dystrophinopathy, dysferlinopathy, and sarcoglycanopathy. We are interested in the relationship between the severity of dystrophic muscle degeneration and the expression of AQP4. Here we compared the AQP4 expression of the limb muscles with that of diaphragms in both mdx and control mice. The dystrophic muscle degeneration, such as rounding profile of cross sectional myofiber shape, dense eosin staining, central nuclei, and endomysial fibrosis in mdx mice, were more marked in diaphragms than in limb muscles. The decrease of AQP4 expression at protein level was more marked in diaphragms than in the limb muscles of mdx mice. However, the expression of AQP4 mRNA in the diaphragms of mdx mice was not reduced in comparison with limb muscles of mdx mice. The present study revealed that AQP4 expression at protein level was correlated with the severity of dystrophic changes in muscle tissues of mdx mice.

Key words: AQP4 expression, protein and RNA levels, limb muscle, diaphragm, mdx mice

I. Introduction

Aquaporin (AQP) 4 is a water selective channel expressed in the surface membranes of various kinds of cells in the different tissues and organs including skeletal muscle [8, 12, 14, 31]. AQP4 interacts with α1-syntrophin, which is one of the members of dystrophin complex, in its PDZ domain, although this is not always the case. Murine X-linked muscular dystrophy (mdx) and Duchenne muscular dystrophy (DMD) are caused by genetically homologous mechanism and both are characterized by a complete absence of dystrophin, although the limb muscles of adult mdx mice exhibit less severe myofiber degeneration and fibrosis than those of DMD limb muscles. Stedman *et al.* [22] reported that the mdx mouse diaphragm showed severe degenerative changes comparable to those of DMD limb muscles. In addition, they reported that the collagen density in mdx diaphragm rose to at least seven times higher than that of control diaphragm and ten times higher than that of mdx hind-limb muscle [22]. In the limb muscles of the milder Becker muscular dystrophy, orthogonal array, which is the morphological feature of AQP4, is less severely depleted in the sarcolemmal plasma membranes of limb muscles than those in Duchenne muscular dystrophy [19]. However, reduced expression of AQP4 was also described in the skeletal muscles with Fukuyama congenital muscular dystrophy (FCMD), sarcoglycanopathy or dysferlinopathy, [2, 3, 30, 31]. Therefore, decreased expression of AQP4 is not always entirely dependent on the absence of dystrophin and other factors may also be involved. To test this bypothesis, we analyzed the degree of AQP4 expression at mRNA and protein levels in mdx diaphragm in comparison with that of mdx limb muscle.

Correspondence to: Yoshihiro Wakayama, M.D., Ph.D., Department of Neurology, Showa University Fujigaoka Hospital, 1–30 Fujigaoka, Aoba-ku, Yokohama 227–8501, Japan.
E-mail: wakayama@med.showa-u.ac.jp

II. Materials and Methods

Animals and tissues

Diaphragms and quadriceps femoris muscles were

excised from normal mice (n=7; *C57BL/6*) aged 3 months, while mdx diaphragms and quadriceps femoris muscles were obtained from age matched mdx mice (n=5; *C57BL/10ScSn-mdx*). The mice were killed by cervical dislocation. All animal experiments were performed in compliance with the NIH Guide for the Care and Use of Laboratory Animals and were approved by the ethics committee of Showa University (admission No. 30005).

Real-time quantitative reverse transcription polymerase chain reaction (Real-time quantitative RT-PCR) for mouse AQP4

Total RNA was extracted from approximately 30 mg of diaphragms and quadriceps femoris muscles from 7 normal (*C57BL/6*) mice and 5 mdx (*C57BL/10ScSn-mdx*) mice with an acid-phenol extraction reagent (TRIzol, code 15596-026; Gibco BRL, Rockville, MD, USA). The concentration of AQP4 mRNA content was estimated by real-time quantitative RT-PCR as described previously [20]. The oligonucleotide primers were designed from the mouse AQP4 sequence (Entrez U88623): sense strand, 5'-GAAAACCCCTTACCTGTGG-3'; antisense strand, 5'-AGCTGGCAAAAATAGTGA-3'. To compensate for differences in the RNA quality or RT efficacy, the expression of the glyceraldehyde-3 phosphate dehydrogenase (G3PDH) gene was quantified as housekeeping gene in each sample. The oligonucleotide primers for G3PDH were designed according to the manufacturer's catalog (Clontech Laboratories Inc., Mountain View, CA, USA): sense strand, 5'-ACCACAGTCCATGCCATCAC-3'; antisense strand, 5'-TCCACCACCCTGTTGCTGTA-3'.

For the generation of standard curves of AQP4 and G3PDH, we synthesized primers by adding T7 promoter sequence to forward primer and oligo-dT sequence to reverse primer for both AQP4 and G3PDH genes. The total RNAs 100 ng (1 μl of 100 ng/μl) extracted from mouse skeletal muscles were reverse transcribed and amplified by PCR using one step RNA PCR Kit (TaKaRa Bio Inc., Shiga, Japan, Code RR024A). After gel electrophoresis of the RT-PCR products, the bands corresponding to AQP4 and G3PDH cDNAs were extracted and purified. Using these double stranded DNA as templates, single stranded RNA was made using In Vitro Transcription T7 Kit (TaKaRa Bio Inc., Code 6140) and copy number was calculated both in AQP4 and G3PDH products. The samples of serial dilution were made with respect to AQP4 and G3PDH RNAs. Before making the standard curve for AQP4 mRNA, the single stranded mouse AQP4 mRNA was denatured at 70°C for 10 min and the gel electrophoresis was performed with 1.87 μg of denatured RNA in 2.5% agarose gel. After confirming the purity of the single stranded AQP4 mRNA, the diluted samples were reverse transcribed for 10 min at 50°C followed by 25 cycles of PCR (30 sec and 20 sec at 94°C and 48°C, respectively, and 30 sec at 72°C) with the reaction mixture containing 1×PCR buffer, 0.4 μM each of primer pairs, 5 mM magnesium chloride, 0.8 U/μl ribonuclease inhibitor, 0.1 U/μl reverse transcriptase, 0.1 U/μl Taq polymerase and 1 mM dNTP mixture using Real Time One Step RNA PCR Kit (TaKaRa Bio Inc., Code RR026A) and Smart Cycler (Cepheid, CA, USA). For the calculation of the copy numbers of AQP4 mRNAs, the extracted RNA samples were reverse transcribed and the resultant cDNAs were amplified by PCR similarly. For making the standard curve for G3PDH mRNA and the calculation of the copy numbers of G3PDH mRNAs, the samples were reverse transcribed for 10 min at 50°C followed by 30 cycles of PCR (30 sec and 20 sec at 94°C and 62°C, respectively, and 30 sec at 72°C) in the same reaction mixture described above. Based on the standard curve, the copy numbers of mRNAs of G3PDH were calculated. Finally the ratio of AQP4 mRNA copy number versus G3PDH mRNA copy number was calculated in each tissue of normal mice and age-matched mdx mice, and statistically compared by two-tailed t test. Difference between mean values was considered significant when $p<0.05$.

Peptide synthesis and antibody production

General procedures for peptide synthesis and antibody production were performed as previously described [26, 27]. Briefly the peptides (C-EKKGKDSSGEVLSSV [7] and GKKDKEKRFSFFPKKK-C [18, 32] of the C-terminal domains of the rat AQP4 and the human β-spectrin, respectively, were synthesized. Antibodies against these peptides were generated in rabbit. An enzyme-linked immunosorbent assay was used to determine the rabbit polyclonal antibody titers, which were ×204,800 and ×200,000, respectively.

Immunohistochemistry

Quadriceps femoris muscles and diaphragms from 4 normal mice (*C57BL/6*) and 4 mdx mice (*C57BL/10ScSn-mdx*) were obtained after killing mice by cervical dislocation. The excised muscle samples were immediately frozen in isopentane cooled by liquid nitrogen. Six-micrometer-thick frozen transverse sections of muscles were placed on slide glasses and incubated with primary antibodies which included rabbit anti-AQP4 and β-spectrin antibodies [27, 29]. After washing in PBS, the sections were incubated with FITC-conjugated swine anti-rabbit immunoglobulin [26].

The percentages of AQP4 positive myofibers were calculated both in the quadriceps femoris muscles and diaphragm muscles of 4 mdx mice as follows. Serially sectioned muscle specimens with immunohistochemical staining by anti-APQ4 and anti-β-spectrin antibodies, respectively, were photographed. The photographs were printed at a final magnification of ×350 and those of β-spectrin immunostaining were used for the calculation of total myofibers present in the given area, while those of AQP4 immunostaining were used for the estimation of total number of AQP4 positive myofibers in the same area. Here the myofibers with more than 80% surface immunolabeling by anti-AQP4 antibody were defined as the AQP4 positive myofibers. Thus the percentage of AQP4 positive myofibers in each muscle of 4 quadriceps femoris muscles and 4 diaphragm muscles of 4 mdx mice was obtained. The

Table 1. *Real-time quantitative RT-PCR analysis in the quadriceps femoris muscle and diaphragm of wild-type and mdx mice*

		AQP4 mRNA copy number / G3PDH mRNA copy number
Wild-type mice (n=7)	Diaphragm	0.17±0.02*1
	Quadriceps femoris muscle	0.11±0.01*2
Mdx mice (n=5)	Diaphragm	0.12±0.01*3
	Quadriceps femoris muscle	0.01±0.01*4

* Group mean±standard error of the mean
*1 versus *3: p>0.1
*2 versus *4: p<0.01
*1 versus *2: p<0.05
*3 versus *4: p<0.01 (two tailed t-test)

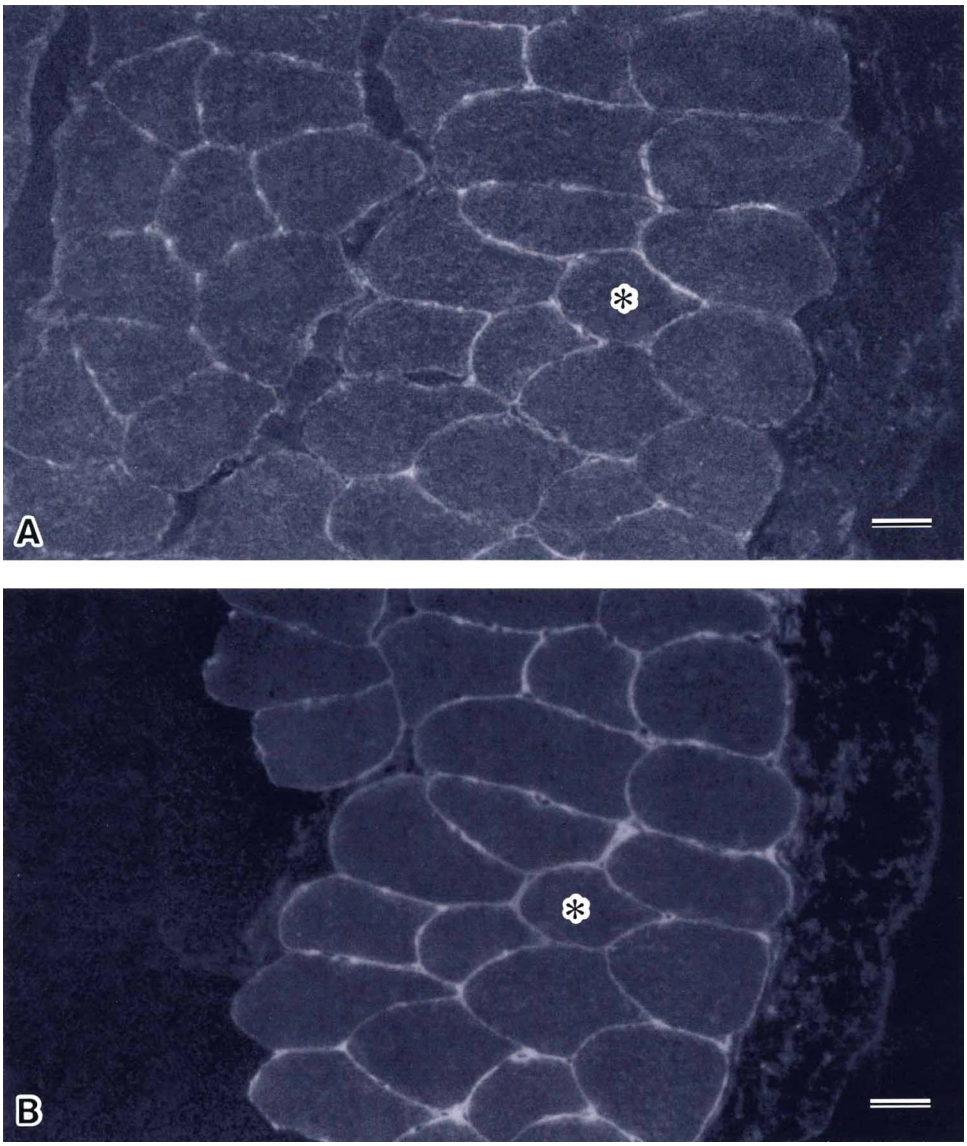

Fig. 1. The immunostaining of serial sections of normal quadriceps femoris muscle with anti-AQP4 (**A**) and β-spectrin (**B**) antibodies. The normal quadriceps femoris myofibers show the basically immunopositive reaction with both antibodies, although the immunoreactivity with anti-AQP4 antibody is a little bit weaker in some myofibers (**A**) in comparison with that of anti-β-spectrin antibody (**B**). The myofiber with asterisk in **A** and **B** is the same myofiber. Bar=20 μm (**A, B** ×400).

difference in the group mean percentages of 4 quadriceps femoris muscles and 4 diaphragm muscles was statistically compared by two tailed t-test. Difference between mean values was considered significant when $p<0.05$.

III. Results

Real-time quantitative RT-PCR of AQP4 mRNA

The relative AQP4 mRNA levels in quadriceps femoris muscles and diaphragms of normal mice were 0.11±0.01 and 0.17±0.02, respectively, while those of mdx mice were 0.01±0.01 and 0.12±0.01, respectively (Table 1). The AQP4 mRNA levels of diaphragms were slightly higher than those of quadriceps femoris muscles in normal mice ($0.01<p<0.05$ by two tailed t-test). However, the AQP4 mRNA levels of quadriceps femoris muscles in mdx mice were significantly lower than those of normal mice ($p<0.01$), although the levels of diaphragms between normal and mdx mice were not ($p>0.1$).

Immunohistochemistry

The immunostaining of normal quadriceps femoris muscles with anti-AQP4 antibody showed most of the myofiber surface membranes were positively stained with this antibody (Fig. 1A). The immunohistochemistry with anti-β-spectrin antibody of serial section of normal quadri-

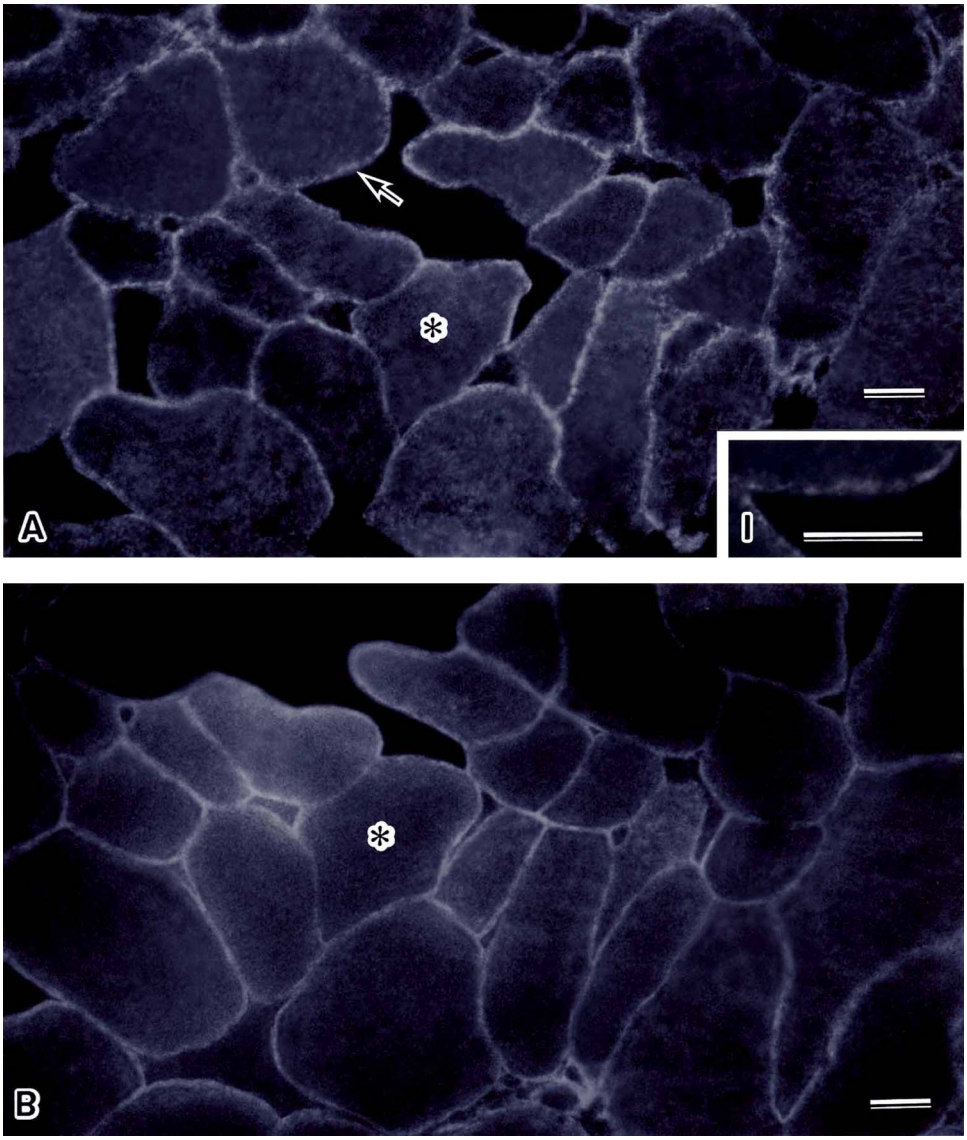

Fig. 2. The immunostaining of serial sections of normal diaphragm muscle with anti-AQP4 (**A**) and β-spectrin (**B**) antibodies. The normal diaphragm myofibers reveal the immunopositive reaction with both antibodies, although the immunoreactivity with anti-AQP4 antibody appears slightly discontinuous in comparison with that of anti-β-spectrin antibody (**B**). Higher magnification of **A** (inset: **I**) shows the dot-like immunoreactivity of myofiber surface membrane with anti-AQP4 antibody. The myofiber with asterisk in **A** and **B** is the same myofiber. Bar=20 μm (**A, B** ×400, **I** ×800).

ceps femoris muscles revealed that the surface membranes of all the myofibers were immunostained continuously with this antibody (Fig. 1B). The normal diaphragm myofibers revealed the immunopositive reaction at the myofiber surface with both anti-AQP4 and β-spectrin antibodies (Fig. 2A, B), although the immunoreactivity with anti-AQP4 antibody appeared to be slightly discontinuous (Fig. 2I).

In the quadriceps femoris muscle sections of mdx mice, the immunoreactivity with anti-AQP4 antibody (Fig. 3A) was reduced in comparison with that of quadriceps femoris muscles of normal mice (Fig. 1A). The mdx quadriceps femoris myofibers showed a negative or partially positive immunoreactivity with anti-AQP4 antibody (Fig. 3A). The immunostaining of mdx quadriceps femoris myofibers with anti-β-spectrin antibody revealed the positive staining in all myofibers (Fig. 3B). In the diaphragm sections of mdx mice, most of the myofibers demonstrated a negative or minimally immunopositive staining with anti-AQP4 antibody (Fig. 4A). The immunonegativity of anti-AQP4 antibody was more marked in mdx diaphragm myofibers (Fig. 4A) in comparison with that of mdx quadriceps femoris myofibers (Fig. 3A). The immunohistochemistry of mdx diaphragm myofibers with anti-β-spectrin antibody showed that most of the mdx diaphragm myofibers were immunopositive with this antibody (Fig. 4B), although the immunoreactivity was somewhat irregular (Fig. 4B).

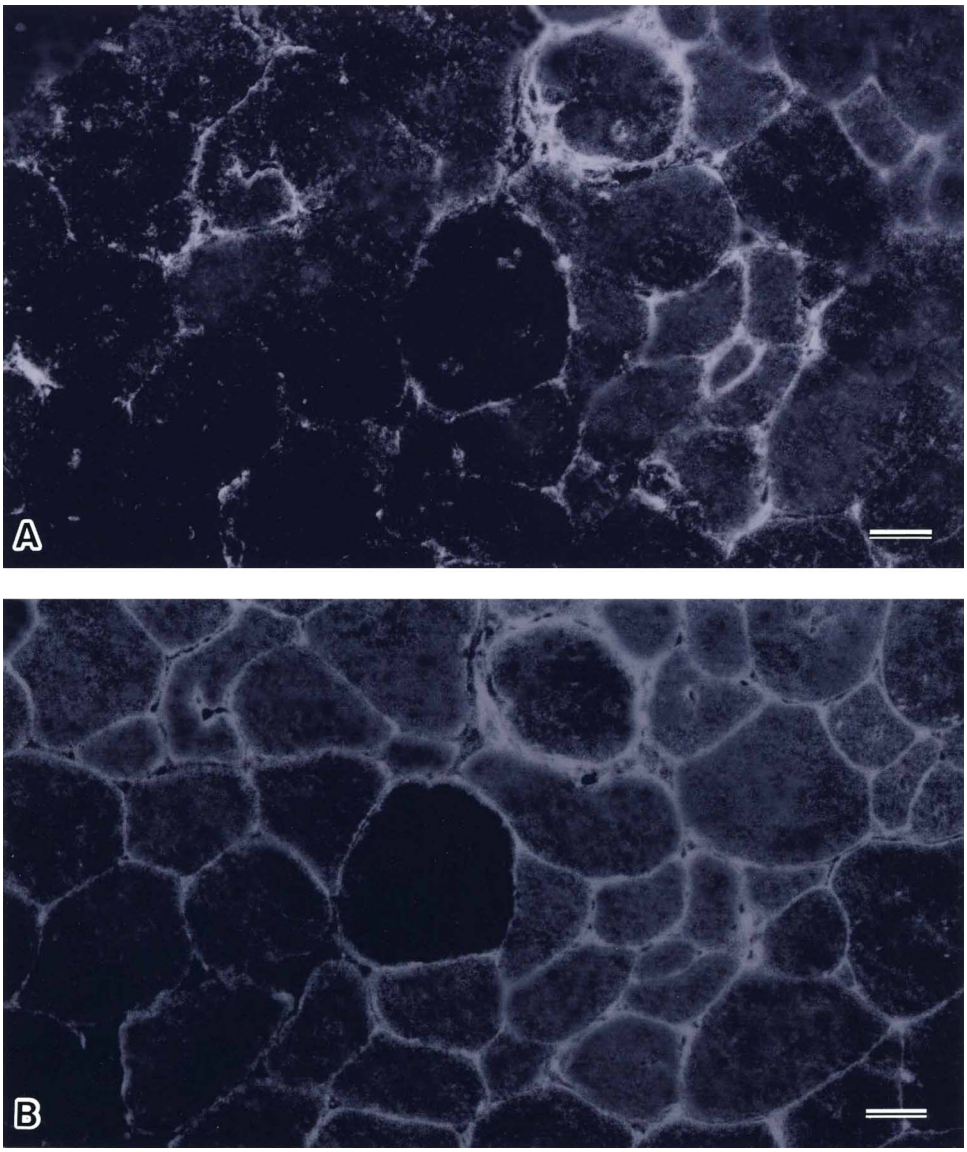

Fig. 3. The immunostaining of serial sections of mdx quadriceps femoris muscle with anti-AQP4 (**A**) and β-spectrin (**B**) antibodies. In the mdx quadriceps femoris muscle sections, the immunoreactivity with anti-AQP4 antibody (**A**) is reduced in comparison with that of normal quadriceps femoris muscle (Fig. 1A) and most of the mdx myofibers show the negative or partially positive immunoreactivity with this antibody (**A**). The immunostaining of mdx quadriceps femoris myofibers with anti-β-spectrin antibody revealed the positive staining in all myofibers (**B**). Bar=20 μm (**A, B** ×400).

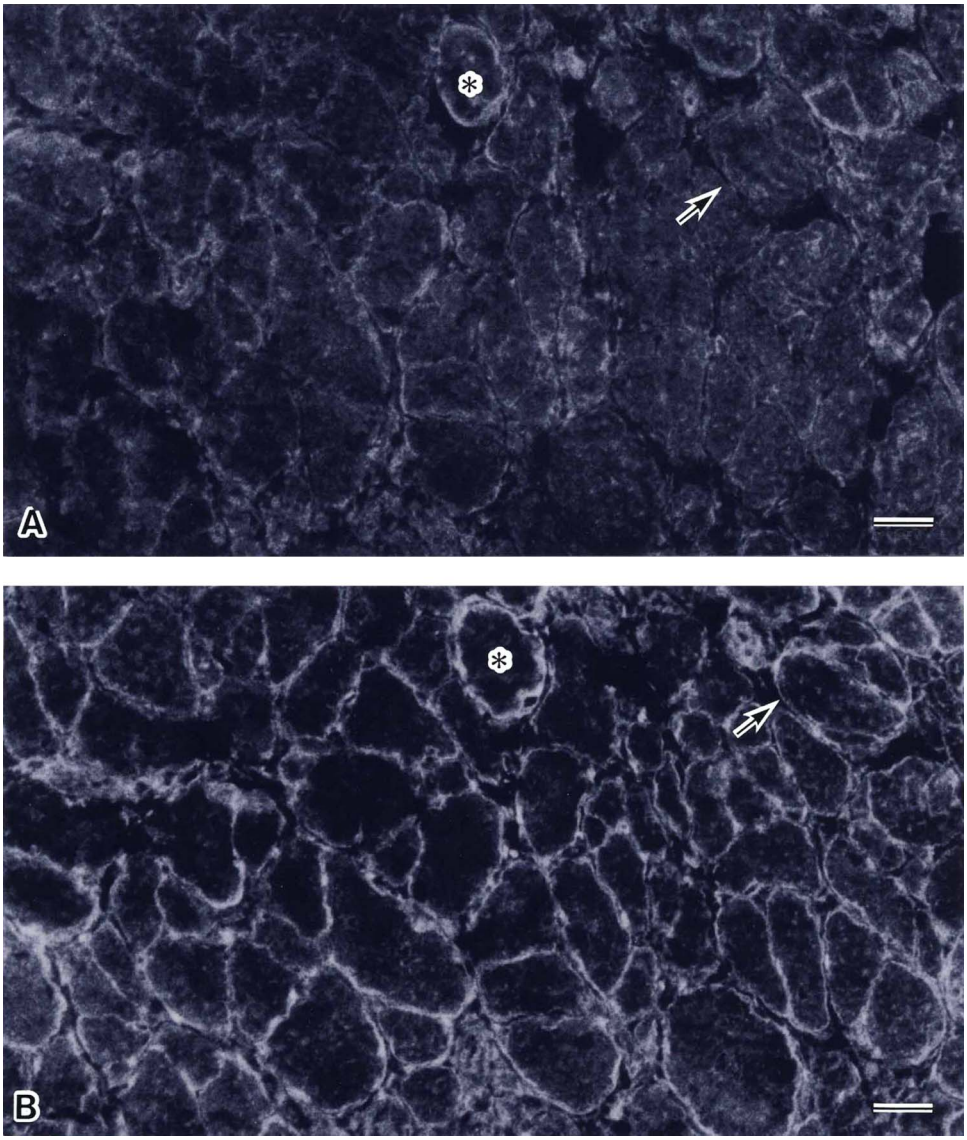

Fig. 4. The immunostaining of serial sections of mdx diaphragm with anti-AQP4 (**A**) and β-spectrin (**B**) antibodies. Most of the mdx diaphragm myofibers demonstrated a negative or minimally immunopositive staining with anti-AQP4 antibody (**A**). The immunonegativity of anti-AQP4 antibody is more marked in mdx diaphragm myofibers in comparison with that of mdx quadriceps femoris myofibers (Fig. 3A). The myofibers indicated by asterisk and arrow (**A** and **B**) reveal that the myofiber with asterisk (**A**) shows the positive AQP4 immunostaining and the myofiber indicated by arrow (**A**) reveals the negative AQP4 immunoreactivity, respectively, although both myofibers are immunopositive with anti-β-spectrin antibody (**B**). The myofiber surface immunoreactivity with anti-β-spectrin antibody was somewhat irregular (**B**). Bar=20 μm (**A, B** ×400).

The semiquantitative study showed that the group mean percentage±standard error of the mean of AQP4 positive myofibers was 19.4±4.2 and 5.8±2.2 in the quadriceps femoris muscles and diaphragm muscles of 4 mdx mice, respectively. These percentages were significantly different ($p<0.03$)

IV. Discussion

Although both mdx mouse and DMD are characterized by a complete absence of dystrophin, the clinical phenotype is rather different and the disability of mdx mouse is very mild. The difference of running ability between mdx and normal mice is difficult to evaluate without using instruments [6]. Pathologically speaking, the limb muscles of mdx mouse reveal milder dystrophic changes than those of DMD. Furthermore, less marked myofiber degeneration and interstitial fibrosis, and more sarcolemmal expression of AQP4 are characteristic features in limb muscle of mdx mice [11]. The pathomechanism of this difference between mdx and DMD muscles is unknown. It is also unclear why the different muscles, such as limb muscle and diaphragm of mdx mouse, show the different degrees of severity of dystrophic changes. Mdx myofibers lack sarcolemmal

dystrophin, which is abundant at the costamere in normal myofibers [13, 15, 17, 23, 28]. Although it is not always the case, AQP4 interacts with α1-syntrophin, one of the members of dystrophin complex, with its postsynaptic density-95, Drosophila disc large protein and the Zona occludens protein I protein-interaction (PDZ) domain [1]. Consequently, the intrinsic membrane protein AQP4 is more abundantly present at the costameres where β-spectrin is also concentrated [18].

Dystrophic myofibers often lack the sarcolemmal plasma membrane [16] where β-spectrin is expressed. In this study β-spectrin immunostaining was performed in order to confirm the presence of sarcolemmal plasma membranes without expressing AQP4 protein in dystrophic mdx mice. Dystrophin-deficient mdx mouse muscle and DMD muscle are thought to lack dystrophin complex, resulting in the absence of α1-syntrophin. This in turn relates to the decreased expression of AQP4 in the muscles of mdx mice and DMD boys. Although decreased, the degree of the reduced expression of AQP4 at protein level is milder in the limb muscle of mdx mouse than in the quadriceps femoris muscle of DMD [11]. However, a substantial amount of AQP4 protein is expressed in mdx quadriceps femoris muscles. This suggests that the AQP4 anchoring proteins other than α1-syntrophin are present at the mdx myofiber surface. At RNA level, a normal level of AQP4 mRNA in mdx muscle was reported [4]. The level of AQP4 mRNA in the diaphragm of mdx mouse was not different statistically from that of normal mouse in the present study, although it was statistically reduced in the quadriceps femoris muscle of mdx mouse in comparison with that of normal mouse. This may be due to more active myofiber degeneration and regeneration in the mdx diaphragm [24]. Moreover, AQP4 mRNA level analysis of diaphragms and quadriceps femoris muscles of mdx mice implied that AQP4 anchoring proteins other than α1-syntorophin, if present, may also be more markedly reduced in diaphragms than in the quadriceps femoris muscles of mdx mice.

In freeze fracture electron microscopy, a decreased density of orthogonal arrays was observed in the muscles of FCMD which is severe muscular dystrophy [25]. Following this study, we studied the AQP4 expression in the muscles of FCMD with normal dystrophin expression, and reported the decreased expression of AQP4 in the muscles with FCMD [30].

Studies of AQP4 expression in other dystrophic muscles also showed the reduced expression of AQP4 in the muscles with α-dystroglycanopathy [1], dysferlinopathy [2] or sarcoglycanopathy [3]. Au *et al.* [2] suggested that altered AQP4 expression observed in the dystrophic muscle biopsies are likely secondary to the dystrophic process. The present results revealed that the decrease of AQP4 protein was more marked in the diaphragm muscles than in the limb muscles of mdx mice. The immature muscle cells do not express AQP4 at their surface membranes and one of the factors to express AQP4 is nerve influence [9, 10, 21]. The interstitial fibrosis of skeletal muscle tissue is more marked in mdx diaphragm than in mdx limb muscle [22]. Myofibrosis is a complex and incompletely understood process characterized by excessive accumulation of collagen IV and other extracellular matrix components. Excessive collagen accumulation in the mdx diaphragm is associated with dystrophic increase in the expression of transforming growth factor β1 (TGF-β1) without corresponding increase in matrix metalloproteinase-9 (MMP-9) expression [5]. The axonal growth of spinal motor neuronal cells may be inhibited by the interstitial myofibrosis of muscle tissues of mdx mice. Thus, the regenerating myofibers may be more dysinnervated in the mdx diaphragm than in the mdx limb muscle after myofiber degeneration and necrosis. Finally, the present study suggested that the more marked decrease of AQP4 protein observed in the mdx diaphragm muscles are likely secondary to the dystrophic process in addition to the lack of dystrophin.

V. Acknowledgments

The authors wish to express their thanks to Y. Matsuzaki for her technical help. This work was supported by Intramural Research Grant (20B-13) for Neurological and Psychiatric Disorders of NCNP.

VI. Conflict of Interest

All authors of this paper declare that there is no conflict of interest related to the content of this manuscript including employment or personal financial interests.

VII. References

1. Adams, M. E., Mueller, H. A. and Froehner, S. C. (2001) In vivo requirement of the alpha-syntrophin PDZ domain for the sarcolemmal localization of nNOS and aquaporin-4. *J. Cell Biol.* 155; 113–122.
2. Au, C. G., Butler, T. L., Egan, J. R., Cooper, S. T., Lo, H. P., Compton, A. G., North, K. N. and Winlaw, D. S. (2008) Changes in skeletal muscle expression of AQP1 and AQP4 in dystrophinopathy and dysferlinopathy patients. *Acta Neuropathol.* 116; 235–246.
3. Crosbie, R. H., Dovico, S. A., Flanagan, J. D., Chamberlain, J. S., Ownby, C. L. and Campbell, K. P. (2002) Characterization of aquaporin-4 in muscle and muscular dystrophy. *FASEB J.* 16; 943–949.
4. Frigeri, A., Nicchia, G. P., Nico, B., Quondamatteo, F., Herken, R., Roncali, L. and Svelto, M. (2001) Aquaporin-4 deficiency in skeletal muscle and brain of dystrophic mdx mice. *FASEB J.* 15; 90–98.
5. Graham, K. M., Singh, R., Millman, G., Malnassy, G., Gatti, F., Bruemmer, K., Stefanski, C., Curtis, H., Sesti, J. and Carlson, C. G. (2010) Excessive collagen accumulation in dystrophic (mdx) respiratory musculature is independent of enhanced activation of the NF-κB pathway. *J. Neurol. Sci.* 294; 43–50.
6. Hara, H., Nolan, P. M., Scott, M. O., Bucan, M., Wakayama, Y. and Fischbeck, K. H. (2002) Running endurance abnormality in mdx mice. *Muscle Nerve* 25; 207–211.
7. Hasegawa, H., Ma, T., Skach, W., Matthay, M. A. and Verkman, A. S. (1994) Molecular cloning of a mercurial-insensitive water channel expressed in selected water-transporting tissues. *J. Biol.*

Chem. 269; 5497–5500.
8. Iida, Y., Matsuzaki, T., Morishima, T., Sasano, H., Asai, K., Sobue, K. and Takata, K. (2009) Localization of reversion-induced LIM protein (RIL) in the rat central nervous system. *Acta Histochem. Cytochem.* 42; 9–14.
9. Jimi, T. and Wakayama, Y. (1990) Effect of denervation on regenerating muscle plasma membrane integrity: freeze-fracture and dystrophin immunostaining analyses. *Acta Neuropathol.* 80; 401–405.
10. Jimi, T., Wakayama, Y., Matsuzaki, Y., Hara, H., Inoue, M. and Shibuya, S. (2004) Reduced expression of aquaporin 4 in human muscles with amyotrophic lateral sclerosis and other neurogenic atrophies. *Pathol. Res. Pract.* 200; 203–209.
11. Liu, J. W., Wakayama, Y., Inoue, M., Shibuya, S., Kojima, H., Jimi, T. and Oniki, H. (1999) Immunocytochemical studies of aquaporin 4 in the skeletal muscle of mdx mouse. *J. Neurol. Sci.* 164; 24–28.
12. Masaki, H., Wakayama, Y., Hara, H., Jimi, T., Unaki, A., Iijima, S., Oniki, H., Nakano, K., Kishimoto, K. and Hirayama, Y. (2010) Immunocytochemical studies of aquaporin 4, Kir4.1, and α1-syntrophin in the astrocyte endfeet of mouse brain capillaries. *Acta Histochem. Cytochem.* 43; 99–105.
13. Masuda, T., Fujimaki, N., Ozawa, E. and Ishikawa, H. (1992) Confocal laser microscopy of dystrophin localization in guinea pig skeletal muscle fibers. *J. Cell Biol.* 119; 543–548.
14. Matsuzaki, T., Hata, H., Ozawa, H. and Takata, K. (2009) Immunohistochemical localization of the aquaporins AQP1, AQP3, AQP4, and AQP5 in the mouse respiratory system. *Acta Histochem. Cytochem.* 42; 159–169.
15. Minetti, C., Beltrame, F., Marcenaro, G. and Bonilla, E. (1992) Dystrophin at the plasma membrane of human muscle fibers shows a costameric localization. *Neuromuscul. Disord.* 2; 99–109.
16. Mokri, B. and Engel, A. (1975) Duchenne dystrophy: electron microscopic findings pointing to a basic or early abnormality in the plasma membrane of the muscle fiber. *Neurology* 25; 1111–1120.
17. Pardo, J. V., Siliciano, J. D. and Craig, S. W. (1983) A vinculin-containing cortical lattice in skeletal muscle: transverse lattice elements ("costameres") mark sites of attachment between myofibrils and sarcolemma. *Proc. Natl. Acad. Sci. U S A* 80; 1008–1012.
18. Porter, G. A., Dmytrenko, G. M., Winkelmann, J. C. and Bloch, R. J. (1992) Dystrophin colocalizes with β-spectrin in distinct subsarcolemmal domains in mammalian skeletal muscle. *J. Cell Biol.* 117; 997–1005.
19. Shibuya, S., Wakayama, Y., Jimi, T., Oniki, H., Kobayashi, T., Misugi, N., Kumagai, T., Hasegawa, O., Suzuki, Y. and Kuroiwa, Y. (1994) Freeze-fracture analysis of muscle plasma membrane in Becker's muscular dystrophy. *Neuropathol. Appl. Neurobiol.* 20; 487–494.
20. Shibuya, S., Hara, H., Wakayama, Y., Inoue, M., Jimi, T. and Matsuzaki, Y. (2008) Aquaporin 4 mRNA levels in neuromuscular tissues of wild-type and dystrophin-deficient mice. *Tohoku J. Exp. Med.* 215; 313–319.
21. Sirken, S. M. and Fischbeck, K. H. (1985) Freeze-fracture studies of denervated and tenotomized rat muscle. *J. Neuropathol. Exp. Neurol.* 44; 147–155.
22. Stedman, H. H., Sweeney, H. L., Shrager, J. B., Maguire, H. C., Panettieri, R. A., Petrof, B., Narusawa, M., Leferovich, J. M., Sladky, J. T. and Kelly, A. M. (1991) The mdx mouse diaphragm reproduces the degenerative changes of Duchenne muscular dystrophy. *Nature* 352; 536–539.
23. Straub, V., Bittner, R. E., Léger, J. J. and Voit, T. (1992) Direct visualization of the dystrophin network on skeletal muscle fiber membrane. *J. Cell Biol.* 119; 1183–1191.
24. Tanabe, Y., Esaki, K. and Nomura, T. (1986) Skeletal muscle pathology in X chromosome-linked muscular dystrophy (mdx) mouse. *Acta Neuropathol.* 69; 91–95.
25. Wakayama, Y., Kumagai, T. and Shibuya, S. (1985) Freeze-fracture studies of muscle plasma membrane in Fukuyama-type congenital muscular dystrophy. *Neurology* 35; 1587–1593.
26. Wakayama, Y., Jimi, T., Takeda, A., Misugi, N., Kumagai, T., Miyake, S. and Shibuya, S. (1990) Immunoreactivity of antibodies raised against synthetic peptide fragments predicted from mid portions of dystrophin cDNA. *J. Neurol. Sci.* 97; 241–250.
27. Wakayama, Y., Shibuya, S., Takeda, A., Jimi, T., Nakamura, Y. and Oniki, H. (1995) Ultrastructural localization of the C-terminus of the 43-kd dystrophin-associated glycoprotein and its relation to dystrophin in normal murine skeletal myofiber. *Am. J. Pathol.* 146; 189–196.
28. Wakayama, Y., Kojima, H., Inoue, M., Murahashi, M., Shibuya, S., Takahashi, J. and Oniki, H. (2001) Confocal laser and immunoelectron microscopic studies of aquaporin 4 localization in normal skeletal myofiber. *Acta Myologica* 20; 125–129.
29. Wakayama, Y., Jimi, T., Inoue, M., Kojima, H., Murahashi, M., Kumagai, T., Yamashita, S., Hara, H. and Shibuya, S. (2002) Reduced aquaporin 4 expression in the muscle plasma membrane of patients with Duchenne muscular dystrophy. *Arch. Neurol.* 59; 431–437.
30. Wakayama, Y., Jimi, T., Inoue, M., Kojima, H., Yamashita, S., Kumagai, T., Murahashi, M., Hara, H. and Shibuya, S. (2003) Altered aquaporin 4 expression in muscles of Fukuyama-type congenital muscular dystrophy. *Virchows Arch.* 443; 761–767.
31. Wakayama, Y. (2010) Aquaporin expression in normal and pathological skeletal muscles: a brief review with focus on AQP4. *J. Biomed. Biotechnol.* 2010; 731569.
32. Winkelmann, J. C., Costa, F. F., Linzie, B. L. and Forget, B. G. (1990) β Spectrin in human skeletal muscle: tissue-specific differential processing of 3' β-spectrin isoform with a unique carboxyl terminus. *J. Biol. Chem.* 265; 20449–20454.